Phosphatidylserine translocation at the yeast *trans*-Golgi network regulates protein sorting into exocytic vesicles

Hannah M. Hankins[a], Yves Y. Sere[b], Nicholas S. Diab[a], Anant K. Menon[b], and Todd R. Graham[a]
[a]Department of Biological Sciences, Vanderbilt University, Nashville, TN 37235; [b]Department of Biochemistry, Weill Cornell Medical College, New York, NY 10065

ABSTRACT **Sorting of plasma membrane proteins into exocytic vesicles at the yeast *trans*-Golgi network (TGN) is believed to be mediated by their coalescence with specific lipids, but how these membrane-remodeling events are regulated is poorly understood. Here we show that the ATP-dependent phospholipid flippase Drs2 is required for efficient segregation of cargo into exocytic vesicles. The plasma membrane proteins Pma1 and Can1 are missorted from the TGN to the vacuole in *drs2Δ* cells. We also used a combination of flippase mutants that either gain or lose the ability to flip phosphatidylserine (PS) to determine that PS flip by Drs2 is its critical function in this sorting event. The primary role of PS flip at the TGN appears to be to control the oxysterol-binding protein homologue Kes1/Osh4 and regulate ergosterol subcellular distribution. Deletion of *KES1* suppresses plasma membrane–missorting defects and the accumulation of intracellular ergosterol in *drs2* mutants. We propose that PS flip is part of a homeostatic mechanism that controls sterol loading and lateral segregation of protein and lipid domains at the TGN.**

Monitoring Editor
Patrick J. Brennwald
University of North Carolina

Received: Jul 15, 2015
Revised: Oct 2, 2015
Accepted: Oct 6, 2015

INTRODUCTION

The *trans*-Golgi network (TGN) serves as a major sorting station for the delivery of post-Golgi cargo to different subcellular locations (Gu *et al.*, 2001; Papanikou and Glick, 2014). Cargo proteins traveling through the TGN are sorted into exocytic vesicles destined for the plasma membrane or are sorted into vesicles targeted to the endosomal system. Sphingolipid synthesis occurs in the Golgi, and lipids are also sorted at the TGN to produce exocytic vesicles enriched in sphingolipid and sterol relative to the TGN donor membrane (Klemm *et al.*, 2009). Whereas many of the cargoes leaving the TGN for endosomes are sorted by coat-dependent mechanisms (Robinson, 2004), exocytic vesicles enriched in sterol and sphingolipids do not associate with any known coat (Klemm *et al.*, 2009; Surma *et al.*, 2012). Lipid-dependent protein sorting ("lipid raft"–based sorting) has been proposed to explain how specific cargoes are sorted into these vesicles; however, the mechanisms and proteins involved in this sorting process are not well understood (Simons and van Meer, 1988; Simons and Ikonen, 1997; Ikonen and Simons, 1998; Graham and Burd, 2011; Surma *et al.*, 2012). Several candidate proteins have been proposed to be involved in the sorting of cargo into exocytic vesicles, including the budding yeast oxysterol-binding protein (OSBP) homologue Kes1/Osh4 (hereafter referred to as Kes1), which was previously identified in a screen for proteins involved in efficient exocytosis of plasma membrane proteins (Proszynski *et al.*, 2005).

OSBP and Kes1 have been proposed to mediate the unidirectional transport of endoplasmic reticulum (ER) sterol to the TGN, where it is exchanged for Golgi phosphatidylinositol-4-phosphate (PI4P), thereby enriching sterol at the TGN (or directly at exocytic vesicles; Im *et al.*, 2005; Mesmin *et al.*, 2013; von Filseck *et al.*, 2015). The cycle is completed by delivery of PI4P to the ER, where it is converted to phosphatidylinositol (PI) by the phosphatase Sac1 (Mesmin *et al.*, 2013). Genetic studies have implicated *KES1* as a negative regulator of TGN function in exocytosis (Jiang *et al.*, 1994; Fang *et al.*, 1996; Li *et al.*, 2002; Alfaro *et al.*, 2011) and shown that

This article was published online ahead of print in MBoC in Press (http://www.molbiolcell.org/cgi/doi/10.1091/mbc.E15-07-0487) on October 14, 2015.
Address correspondence to: Todd R. Graham (tr.graham@vanderbilt.edu).
Abbreviations used: DHE, dehydroergosterol; Lat A, latrunculin A; OSBP, oxysterol-binding protein; PE, phosphatidylethanolamine; PI, phosphatidylinositol; PI4P, phosphatidylinositol-4-phosphate; PS, phosphatidylserine.
© 2015 Hankins *et al.* This article is distributed by The American Society for Cell Biology under license from the author(s). Two months after publication it is available to the public under an Attribution–Noncommercial–Share Alike 3.0 Unported Creative Commons License (http://creativecommons.org/licenses/by-nc-sa/3.0).
"ASCB®," "The American Society for Cell Biology®," and "Molecular Biology of the Cell®" are registered trademarks of The American Society for Cell Biology.

Kes1 acts in a mutually antagonistic manner with the phospholipid flippase Drs2 (Muthusamy *et al.*, 2009). However, the effect of the relationship between the OSBP homologue Kes1 and the flippase Drs2 on the sorting of proteins into exocytic vesicles, in which ergosterol is highly enriched, is unclear.

There are five yeast flippases in the type IV P-type ATPase family: Neo1, Dnf1, Dnf2, Dnf3, and Drs2. This essential group of flippases generate and maintain plasma membrane asymmetry with phosphatidylserine (PS) and phosphatidylethanolamine (PE) primarily in the cytosolic leaflet and phosphatidylcholine and sphingolipids primarily in the outer (extracellular) leaflet (Kato *et al.*, 2002; Pomorski *et al.*, 2003; Saito *et al.*, 2004; Chen *et al.*, 2006). The mechanism of phospholipid recognition and translocation has been studied extensively with Drs2 and Dnf1 (Baldridge and Graham, 2012, 2013; Baldridge *et al.*, 2013), which are heterodimers with their β subunits Cdc50 and Lem3, respectively (Saito *et al.*, 2004; Chen *et al.*, 2006; Furuta *et al.*, 2007; Takahashi *et al.*, 2011). Drs2 localizes to the TGN and appears to be the primary PS flippase in the cell, but it is also capable of flipping PE (Chen *et al.*, 1999; Hua *et al.*, 2002; Natarajan *et al.*, 2004; Liu *et al.*, 2008; Baldridge *et al.*, 2013). In contrast, Dnf1 dynamically traffics between the plasma membrane, endosomes, and TGN and preferentially flips lysophosphatidylcholine and lysophosphatidylethanolamine (Hua *et al.*, 2002; Pomorski *et al.*, 2003; Riekhof *et al.*, 2007; Baldridge *et al.*, 2013).

Residues defining these differences in substrate specificity have been mapped in Drs2 and Dnf1, and it is possible to tune their substrate preference through targeted mutagenesis. For example, substitution of QQ in the first transmembrane segment of Drs2 for GA (Dnf1 residues) disrupts the ability of Drs2 to flip PS without altering its ability to flip PE (Baldridge and Graham, 2013). Conversely, a N550S point mutation in Dnf1 allows it to flip PS in addition to its normal substrates (Baldridge and Graham, 2013; Baldridge *et al.*, 2013). Surprisingly, Dnf1-N550S, but not wild-type (WT) Dnf1, can replace the function of Drs2 in vivo, indicating that PS flip is the crucial function of Drs2 (Baldridge *et al.*, 2013; Xu *et al.*, 2013).

PS flip by Drs2 was shown to be critical for TGN-associated trafficking pathways (Natarajan *et al.*, 2004; Xu *et al.*, 2013). Drs2 is required for bidirectional transport between the TGN and early endosomes, as well as for the formation of one class of exocytic vesicle; however, loss of Drs2 does not appear to perturb the rate of protein secretion (Chen *et al.*, 1999; Gall *et al.*, 2002; Hua *et al.*, 2002; Liu *et al.*, 2008). Consistent with Drs2's TGN localization, studies by the Grinstein lab using the PS probe Lact-C2 in mammalian cells suggest that PS remains primarily in the lumenal leaflet of the ER and Golgi but gets flipped to the cytosolic leaflet at the TGN (Fairn *et al.*, 2011; Hankins *et al.*, 2015). This change in PS sidedness to the cytosolic leaflet is maintained when TGN-derived vesicles fuse with the plasma membrane, where PS is highly enriched. This finding suggests that the TGN is a major site of PS translocation and also that mammalian cells have PS flippase(s) at the TGN that function similarly to Drs2.

In this study, we investigated how the TGN-localized flippase Drs2 and the OSBP homologue Kes1 are involved in the lipid-based sorting of plasma membrane proteins into exocytic vesicles. To do this, we looked at the distribution of two plasma membrane proteins: the plasma membrane ATPase Pma1 and the arginine transporter Can1. Pma1 and Can1 have been proposed to traffic from the Golgi to the plasma membrane through a lipid-based (coat-independent) mechanism (Bagnat *et al.*, 2000, 2001; Opekarová *et al.*, 2005; Surma *et al.*, 2012). However, once at the plasma membrane, these proteins partition into distinct membrane compartments called the membrane compartments of Pma1 (MCP) and Can1 (MCC; Malínská *et al.*, 2003; Grossmann *et al.*, 2007; Spira *et al.*, 2012; Ziółkowska *et al.*, 2012). We examined the distribution of these proteins both at the plasma membrane and throughout the cell to study the influence of transverse PS asymmetry on exocytic trafficking and lateral compartmentalization of the plasma membrane.

RESULTS

Compartmentalization of the plasma membrane is significantly perturbed in *cho1*Δ cells but not *drs2*Δ cells

To first determine whether plasma membrane organization is perturbed in *drs2*Δ cells, we examined the segregation of Pma1–red fluorescent protein (RFP) and Can1–green fluorescent protein (GFP) into their respective compartments at the cell surface (Figure 1). In WT cells, Pma1-RFP and Can1-GFP colocalized little (Pearson's coefficient = –0.0044 ± 0.023) as previously reported (Malínská *et al.*, 2003; Spira *et al.*, 2012). There was a small increase in colocalization of these proteins in *drs2*Δ cells (Pearson's coefficient = 0.030 ± 0.025) but not significantly so. This result suggests that PS asymmetry is not critical for the normal segregation of MCP and MCC at the plasma membrane. Because we did not see a strong defect when PS asymmetry was disrupted, we also examined whether the absence of PS would have an effect on compartmentalization. To do this, we also imaged *cho1*Δ cells, which are unable to synthesize PS because they lack the PS synthase and must be supplemented with choline to be viable (Atkinson *et al.*, 1980). There was a significant increase in

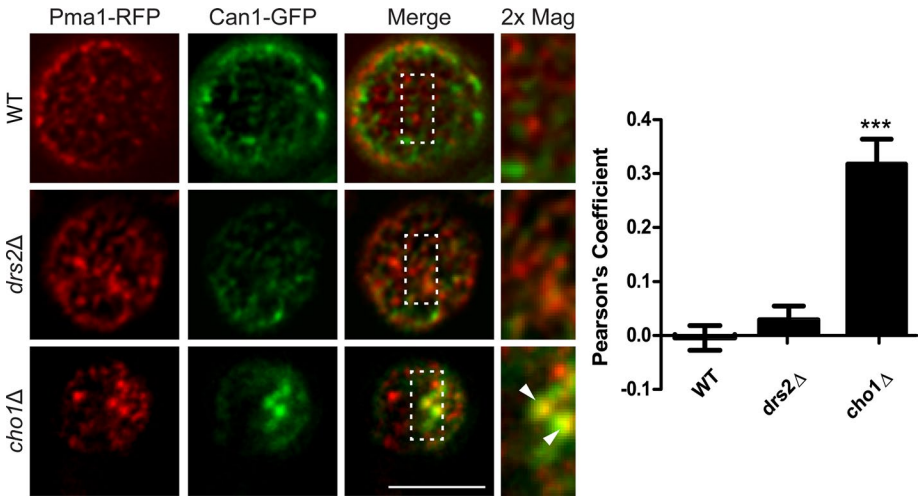

FIGURE 1: Plasma membrane compartmentalization is significantly perturbed in *cho1*Δ cells but not *drs2*Δ cells. Cells expressing Pma1-RFP and Can1-GFP were grown to mid log phase and imaged on a DeltaVision Elite Imaging system. Optical sections were collected every 200 nm. Images were deconvolved using the DeltaVision software SoftWoRx. Arrowheads denote regions of colocalization. Colocalization of the two markers was determined using the ImageJ plug-in Colocalization Finder on deconvolved images. Values represent mean ± SEM (10 cells, one-way analysis of variance [ANOVA], ***$p < 0.001$). Scale bar, 5 μm.

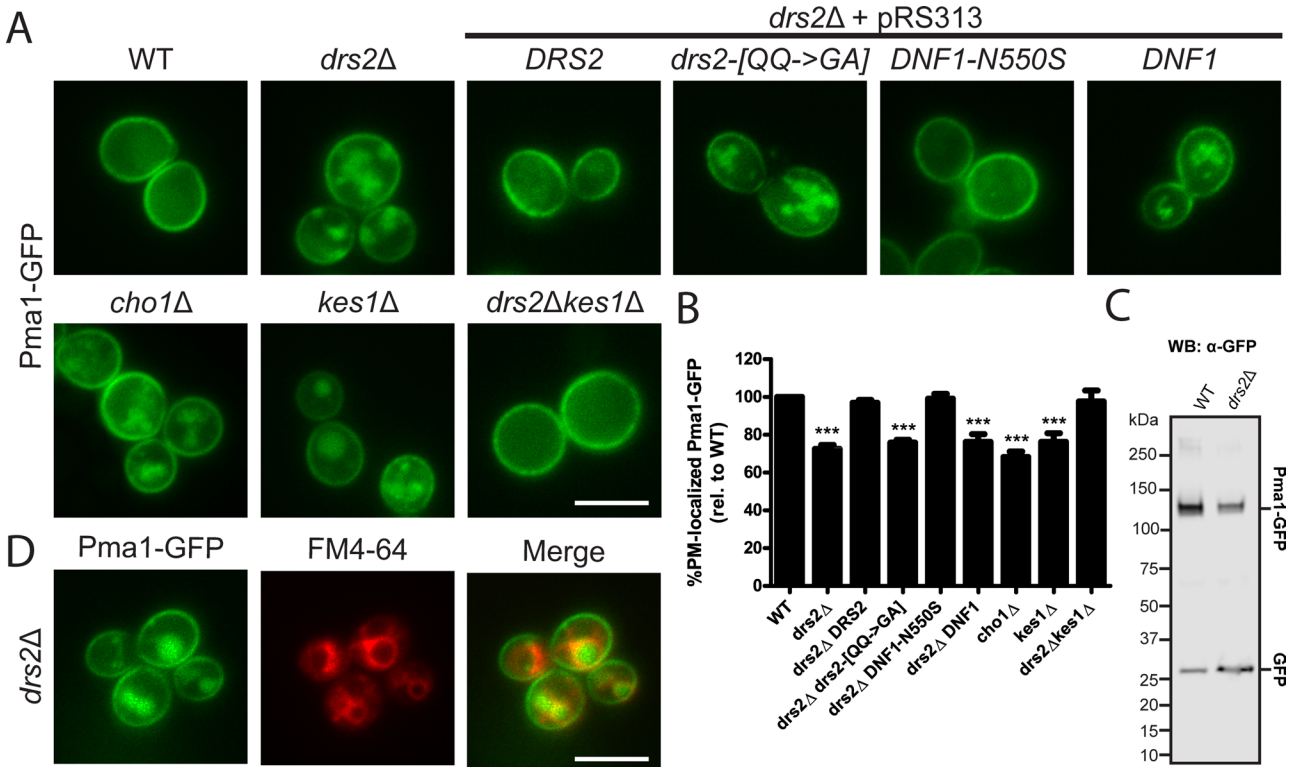

FIGURE 2: Pma1-GFP mislocalizes to the vacuole when TGN PS flippase activity or sterol loading is disrupted. (A) Cells expressing Pma1-GFP were grown to mid log phase at 30°C and imaged. (B) Percentage of PM-localized Pma1-GFP was calculated by dividing plasma membrane fluorescence by total fluorescence with WT set to 100%. Values represent mean ± SEM ($n = 3$, total of 150 cells, one-way ANOVA, ***$p < 0.001$). (C) WT and *drs2*Δ cells expressing Pma1-GFP were probed with anti-GFP antibody. Bands corresponding to full-length Pma1-GFP (127 kDa) and soluble GFP (27 kDa) are indicated on the right. (D) To confirm vacuolar localization, mid log-phase cells were labeled with FM4-64 for 20 min. Scale bar, 5 μm.

colocalization between Pma1-RFP and Can1-GFP in *cho1*Δ cells (Pearson's coefficient = 0.32 ± 0.047), suggesting that the absence of PS has a stronger disrupting effect on distinct membrane compartments at the plasma membrane than loss of PS asymmetry.

Pma1 and Can1 mislocalize to the vacuole when PS flippase activity is disrupted

Although there was not a significant defect in plasma membrane compartmentalization in *drs2*Δ cells (Figure 1), we did observe that the markers were accumulating internally. Pma1-GFP primarily localized to the plasma membrane in WT cells. However, a significant amount of Pma1-GFP mislocalized in *drs2*Δ cells (~25% reduction in plasma membrane fluorescence relative to WT cells; Figure 2, A and B). We determined that the internal Pma1-GFP was accumulating in the vacuole lumen by labeling the cells with FM4-64, which labels the vacuole limiting membrane (Figure 2D). When missorted to the vacuole, Pma1 has been found to enter the vacuole lumen, where it is degraded by vacuolar proteases (Chang and Fink, 1995; Luo and Chang, 2000; Gaigg *et al.*, 2006). In addition, several GFP-tagged membrane proteins have been observed to sort to the vacuolar lumen through the multivesicular body pathway, where GFP remains stable as the remainder of the fusion protein is degraded (Odorizzi *et al.*, 1998; Prosser *et al.*, 2010). Consistent with these observations, the increased Pma1-GFP fluorescence in the vacuole lumen of *drs2Δ* relative to WT cells corresponds to a reduction in the full-length fusion protein and an increase in soluble GFP. In WT cells, 26.0 ± 4.7% of Pma1-GFP is degraded into soluble GFP, whereas 44.5 ± 4.0% of Pma1-GFP is degraded in *drs2*Δ cells as detected by Western blotting with anti-GFP antibody (Figure 2C).

Drs2 primarily flips PS and to a lesser extent PE, and so to distinguish which substrate is important for Pma1-GFP trafficking, we used two flippase mutants that specifically lose (Drs2-[QQ → GA]) or gain (Dnf1-N550S) the ability to flip PS (Baldridge and Graham, 2013). Dnf1-N550S, but not Drs2-[QQ → GA], was able to restore WT-like Pma1 localization to the plasma membrane in *drs2*Δ cells (Figure 2, A and B). This restoration was not due to adding an extra copy of *DNF1*, as *drs2*Δ *DNF1* cells mislocalized Pma1-GFP comparably to *drs2*Δ cells. This finding suggests that PS flip is critical for normal localization of Pma1 at the plasma membrane. Consistently, Pma1 also mislocalized to the vacuole in *cho1*Δ cells (~30% reduction in plasma membrane fluorescence), which are unable to synthesize PS. The same results were observed for Can1 (Figure 3, A–C), although the vacuolar mislocalization defect was stronger for Can1-GFP (~40% reduction in plasma membrane fluorescence; Figure 3, A and B) than Pma1-GFP (~25% reduction in plasma membrane fluorescence; Figure 2, A and B). These observations suggest that PS translocation across the TGN membrane is required for efficient sorting of Pma1-GFP and Can1-GFP to the plasma membrane.

Drs2 and Kes1 work antagonistically in the sorting of Pma1 and Can1

We observed the same antagonistic relationship between *drs2*Δ and *kes1*Δ in sorting plasma membrane proteins that has been described previously for ergosterol homeostasis (Muthusamy *et al.*, 2009). Pma1 and Can1 mislocalized to the vacuole in both *drs2*Δ and *kes1*Δ

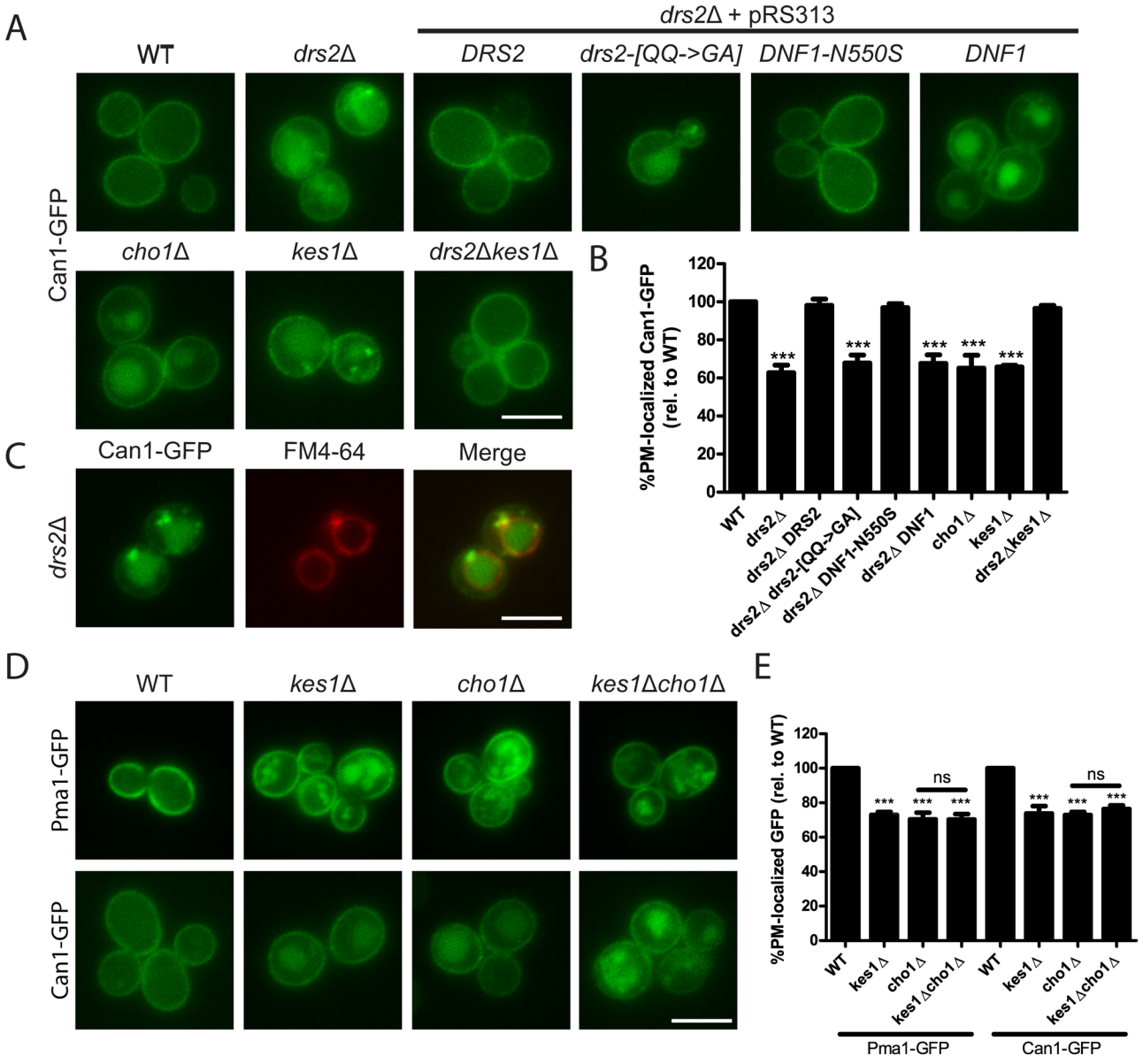

FIGURE 3: Can1-GFP mislocalizes to the vacuole when TGN PS flippase activity or Kes1 activity is disrupted. (A) Cells expressing Can1-GFP were grown to mid log phase at 30°C and imaged. (C) To confirm vacuolar localization, mid log-phase cells were labeled with FM4-64. Scale bar, 5 μm. (D) Deletion of *kes1*Δ does not suppress *cho1*Δ defects in Pma1-GFP or Can1-GFP trafficking. (B, E) Percentage of PM-localized GFP was calculated by dividing PM fluorescence by total fluorescence with WT set to 100%. Values represent mean ± SEM ($n = 3$, total of 150 cells, one-way ANOVA, ***$p < 0.001$). Scale bar, 5 μm.

single mutants but had WT-like distribution in *drs2*Δ*kes1*Δ cells (Figures 2, A–C, and 3, A–C). These results indicate that the activities (or lack of activities) of these two proteins must be matched to facilitate normal trafficking of Pma1 and Can1 to the plasma membrane. Of interest, *kes1*Δ cells did not suppress the *cho1*Δ defect in Pma1 and Can1 mislocalization (Figure 3, D and E), indicating that the presence of PS is required for their efficient plasma membrane localization, and this deficiency cannot be overcome by disrupting *KES1*.

Role of PS in ergosterol enrichment at the plasma membrane

Previously our laboratory showed that Drs2 and Kes1 act antagonistically to regulate sterol distribution between the plasma membrane and internal membranes (Muthusamy *et al.*, 2009). Ergosterol is enriched at the plasma membrane, particularly in the MCC, and is required for correct sorting of Can1 and other plasma membrane permeases (Umebayashi and Nakano, 2003; Malinska *et al.*, 2004; Grossmann *et al.*, 2006, 2007). Therefore we next tested the influence of PS flippases on the cellular distribution of ergosterol to determine whether PS flip is Drs2's critical role in sterol homeostasis.

We first used the fluorescent sterol-binding compound filipin, a polyene antibiotic (Norman *et al.*, 1972; Drabikowski *et al.*, 1973), to observe sterol distribution throughout the cell. Filipin primarily stains the plasma membrane of WT and *drs2*Δ*kes1*Δ cells, but we observed ~20% reduction in filipin staining at the plasma membrane in *drs2*Δ *and kes1*Δ single mutants (Figure 4, A and B), consistent with previous findings (Muthusamy *et al.*, 2009). Transformation of *drs2*Δ

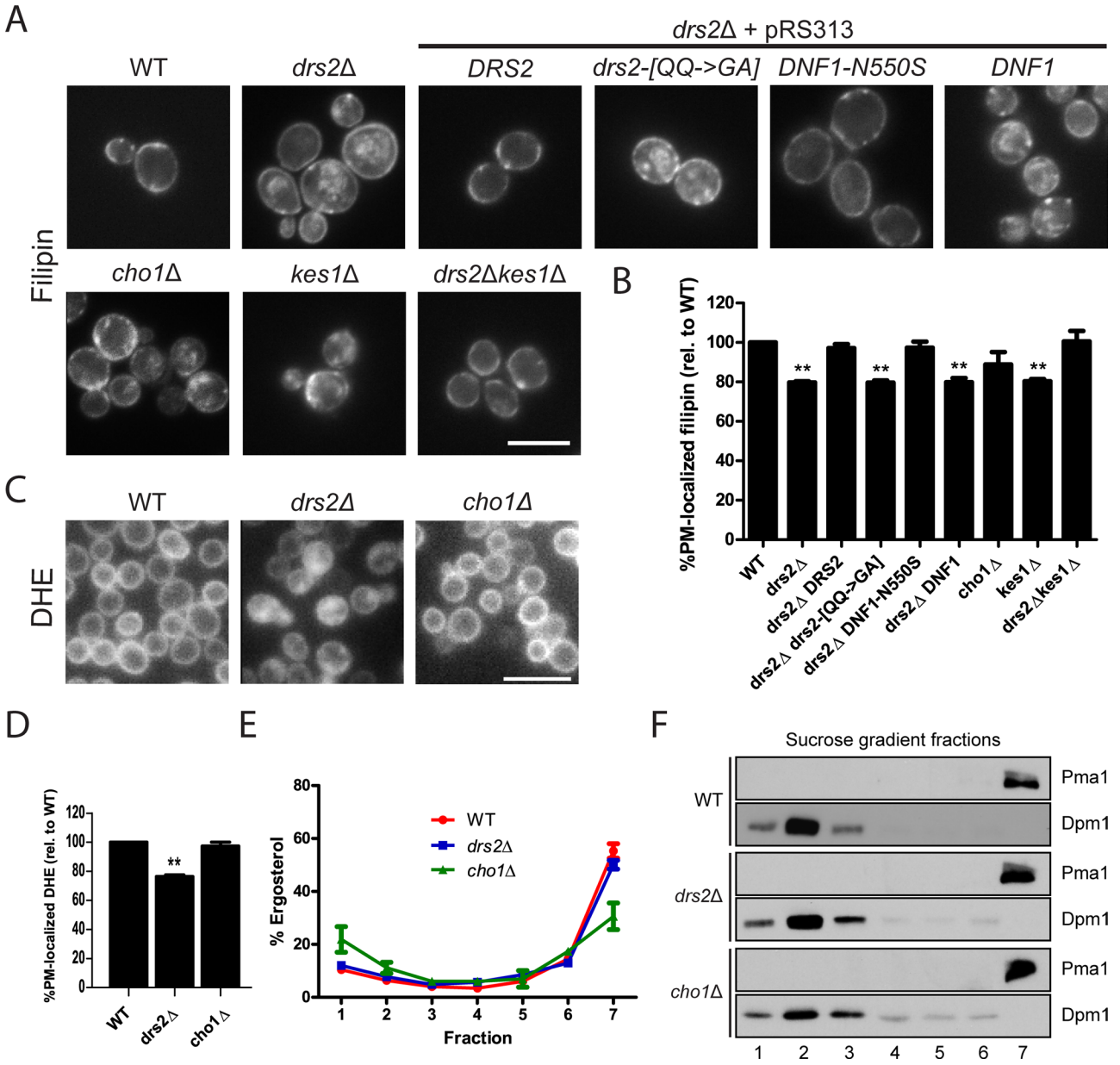

FIGURE 4: Observation of ergosterol distribution in cells using filipin staining, DHE uptake, and sucrose gradient fractionation. (A) Strains were grown at 30°C under aerobic conditions to mid log phase and then fixed with 4% formaldehyde before staining with filipin. (B) Percentage of PM-localized filipin was calculated by dividing PM fluorescence by total fluorescence with WT set to 100%. Values represent mean ± SEM ($n = 3$, total of 150 cells, one-way ANOVA, $^{**}p < 0.01$). Scale bar, 5 μm. (C) Strains were incubated at 30°C under hypoxic conditions for 36 h in the presence of DHE. Scale bar, 10 μm. (D) Percentage of PM-localized DHE was calculated by dividing PM fluorescence by total fluorescence with WT set to 100%. Values represent mean ± SEM ($n = 2$, total of 100 cells, one-way ANOVA, $^{**}p < 0.01$). (E) Strains grown at 30°C under aerobic conditions were subjected to sucrose gradient fractionation, with the lower fractions corresponding to the ER and internal organelles and fraction 7 corresponding to the plasma membrane. (F) Western blots of sucrose gradient fractions from E with Pma1 used as a plasma membrane marker and Dpm1 as an ER marker to verify successful fractionation.

with the *drs2-[QQ → GA]* mutant or WT *DNF1*, which do not recognize PS, failed to correct this defect, and the cells displayed an equivalent 20% reduction in plasma membrane ergosterol. In contrast, WT *DRS2* or *DNF1-N550S*, which can flip PS, completely restored plasma membrane ergosterol in *drs2*Δ cells. The sterol content of *drs2*Δ cells is similar to that in WT cells (Fei *et al.*, 2008), and so these results suggest that PS translocation at the Golgi is required for normal sterol enrichment at the plasma membrane.

Of interest, *cho1*Δ cells had highly variable filipin staining patterns, ranging from a more severe defect than *drs2*Δ to WT-like, even within the same culture. On average, filipin staining of the plasma membrane was reduced in *cho1Δ* cells, but it was not statistically different from that in WT cells (Figure 4, A and B). The *cho1Δ* cells were cultured and imaged under a variety of different conditions, but we were unable to pinpoint the source of variability in the filipin staining pattern. Another potential issue with using

filipin staining as a readout for ergosterol localization is that filipin and other sterol-binding toxins may bind to other molecules or have nonlinear responses to sterol level (Maxfield and Wüstner, 2012).

To try to resolve the variability issues with the *cho1*Δ cells and potential issues intrinsic to filipin staining, we used a second approach to monitor subcellular sterol distribution. We examined cells containing dehydroergosterol (DHE), a fluorescent, naturally occurring sterol that closely mimics ergosterol and is able to functionally replace ergosterol in yeast (Georgiev *et al.*, 2011). Cells were grown under hypoxic conditions for 36 h in medium supplemented with DHE to allow for sterol uptake, which effectively replaces >95% of the ergosterol with DHE (Georgiev *et al.*, 2011). Consistent with the filipin staining, DHE was primarily at the plasma membrane in WT but displayed increased localization to internal structures in *drs2*Δ cells (Figure 4, C and D). Quantitatively, filipin and DHE both indicate ~20% reduction in plasma membrane–localized sterol in *drs2*Δ relative to WT. Therefore filipin appears to provide an accurate measure of ergosterol distribution in *drs2* mutants. Unlike the filipin staining, *cho1*Δ cells were uniformly WT-like, which may be due to differences in growth conditions between the two assays (i.e., growth under aerobic conditions for the filipin stain vs. hypoxic conditions for DHE uptake).

For a third approach to further investigate changes in ergosterol distribution in *cho1*Δ cells, we lysed cells grown under aerobic conditions and separated the plasma membrane from the ER and other internal organelles by fractionation through a sucrose gradient. Ergosterol was quantified in each membrane fraction, and by this assay, 55% of ergosterol in WT cells are at the plasma membrane (fraction 7). Plasma membrane ergosterol of *drs2*Δ cells was reduced to 50%, although this was not statistically different from WT. This lack of statistical significance may be due to the sucrose gradient assay not being sensitive enough to pick up on the relatively small defect observed by filipin staining and DHE fluorescence (the expected result was ~45% ergosterol in the *drs2Δ* plasma membrane fraction). Surprisingly, *cho1Δ* cells displayed a significant depletion of plasma membrane ergosterol (30% of ergosterol in plasma membrane fraction) relative to WT, with a concomitant increase in fractions 1 and 2 corresponding to ER and internal organelles (Figure 4, E and F).

The reason for these discrepancies in the three approaches is not clear, but they may reflect differences in sterol distribution under different growth conditions or the ability of different assays to reproducibly detect small differences in sterol distribution. However, we can conclude that PS is not absolutely required to enrich ergosterol at the plasma membrane because all *cho1Δ* cells lack PS and there are always cells in the population that are indistinguishable from WT when imaged with filipin or DHE. The PS and phosphatidylinositol synthases compete for the same precursor (CDP-diacylglycerol; Kelley *et al.*, 1988), and perhaps increased synthesis of phosphatidylinositol in *cho1Δ* cells can partially compensate for the complete lack of PS. Disruption of *DRS2* does not substantially alter total cellular PS or PI levels (Chen *et al.*, 2006) but instead more subtly perturbs transbilayer PS distribution. In contrast to *cho1Δ*, the *drs2* mutants display a fairly uniform reduction of PM ergosterol as assayed by filipin or DHE and clearly perturb sterol homeostasis.

Pma1 and Can1 are missorted from the TGN to the vacuole in *drs2*Δ and *cho1*Δ cells

We next sought to determine the route by which Pma1 and Can1 travel to the vacuole in the *drs2Δ* and *cho1Δ* mutants. The observed vacuolar mislocalization phenotype could be due to either increased endocytosis at the plasma membrane or misrouting of newly synthesized Pma1 and Can1 from the TGN to the vacuole through the endosomal system. To differentiate these two possibilities for Pma1, we used the actin polymerization inhibitor latrunculin A (Lat A) to block endocytosis (Huang and Chang, 2011). As a positive control, we also imaged GFP-Snc1, an exocytic vesicle–soluble *N*-ethylmaleimide–sensitive factor attachment protein receptor that constantly cycles between the TGN, plasma membrane, and early endosomes (Lewis *et al.*, 2000; Galan *et al.*, 2001).

In WT cells, Snc1 localizes to the bud plasma membrane because endocytosis is the slowest step of Snc1 recycling. In contrast, Snc1 accumulates intracellularly in the early endosomes of *drs2*Δ and *cho1*Δ cells, which have defects in Snc1 recycling (Hua *et al.*, 2002; Furuta *et al.*, 2007; Xu *et al.*, 2013). However, because newly synthesized Snc1 travels to the plasma membrane before arrival in the early endosomes, it will accumulate at the plasma membrane when endocytosis is blocked. After 3 h of Lat A treatment, we found that GFP-Snc1 accumulated significantly more at the plasma membrane in all of the strains, indicating that Lat A was effectively blocking endocytosis (Figure 5, A and B). In contrast, Lat A treatment did not shift the distribution of Pma1-GFP to the plasma membrane in *drs2*Δ and *cho1*Δ cells (Figure 5, A and C). This observation suggests that Pma1-GFP is missorted directly from the TGN rather than being endocytosed from the plasma membrane.

To determine whether Can1 was missorted at the level of the TGN or plasma membrane, we used an endocytosis-resistant Can1-GFP mutant (Can1^{end}-GFP). Can1^{end}-GFP has three N-terminal lysine residues that have been mutated to arginines (K42R/K45R/K47R). These mutations prevent the protein from undergoing ubiquitin-mediated endocytosis, such that once Can1^{end}-GFP reaches the plasma membrane, it should remain there (Charles Lin and Scott Emr, unpublished observations). Can1-GFP and Can1^{end}-GFP were both mislocalized in *drs2*Δ and *cho1*Δ to the same extent, indicating that Can1 is missorted from the TGN to the vacuole (Figure 5, D and E). To ensure that Can1^{end}-GFP is indeed endocytosis resistant, we induced Can1 endocytosis with 5 mM arginine (Supplemental Figure S1). There was a stark decrease in Can1-GFP, but not Can1^{end}-GFP, fluorescence at the plasma membrane in the presence of the high arginine concentration, confirming that Can1^{end}-GFP is endocytosis resistant. These results indicate that TGN missorting, not endocytosis, is the route by which Can1-GFP is mislocalized to the vacuole in *drs2*Δ and *cho1*Δ cells.

Missorting of Pma1 and Can1 is not due to *drs2*Δ AP-1/Rcy1 trafficking defects

We next examined whether the missorting of Pma1 and Can1 is due to previously described trafficking defects caused by disruption of Drs2 flippase activity. Drs2 is required for AP-1/clathrin trafficking between the TGN and early endosomes (Chen *et al.*, 1999; Liu *et al.*, 2008) and the Rcy1 recycling pathway from the early endosomes to TGN (Hua *et al.*, 2002; Furuta *et al.*, 2007). However, disrupting these two pathways by deleting an AP-1 subunit (*apl4*Δ) or *rcy1*Δ had no effect on Pma1 localization (Figure 6, A and C). Can1 localized normally in *apl4*Δ cells, but there was a small increase in Can1 localization to puncta in *rcy1*Δ cells (Figure 6, B and D). However, the Can1 trafficking defect was very mild in comparison to *drs2*Δ (Figure 3, A and B) and was phenotypically distinct. Therefore it is unlikely that disruption of the Rcy1 recycling pathway is the cause of Pma1 and Can1 missorting to the vacuole in *drs2*Δ cells. In addition, we examined whether disrupting other TGN-associated trafficking pathways would affect Pma1 and Can1 sorting. We disrupted the GGA pathway (*gga1,2*Δ) from the TGN

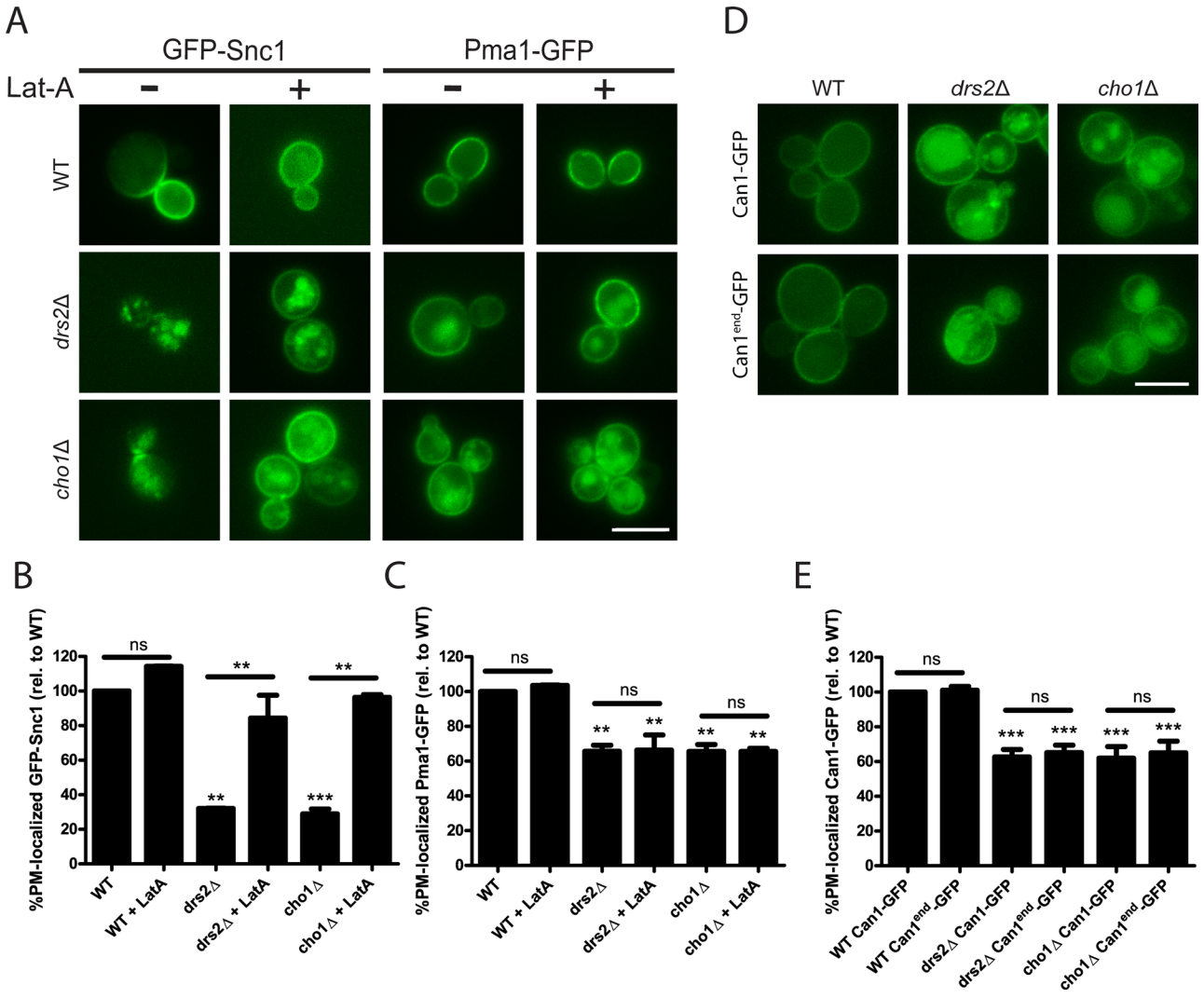

FIGURE 5: Pma1-GFP and Can1-GFP are missorted from the TGN to the vacuole in *drs2*Δ and *cho1*Δ cells. (A) Cells expressing GFP-Snc1 or Pma1-GFP were grown to mid log phase before being switched to medium containing 10 μM Lat A and incubated for 3 h at 30°C. (D) Cells expressing Can1-GFP or endocytosis-resistant Can1^{end}-GFP were grown to mid log phase at 30°C and imaged. (B, C) Values represent mean ± SEM ($n = 2$, total of 100 cells). (E) Values represent mean ± SEM ($n = 3$, total of 150 cells). (B, C, and E) Percentage of PM-localized GFP of the mother cell calculated by dividing plasma membrane fluorescence by total fluorescence with WT set to 100% (one-way ANOVA, $^{**}p < 0.01$, $^{***}p < 0.001$). Scale bar, 5 μm.

to late endosomes and the AP-3 pathway (*apl5*Δ) from the TGN to the vacuole but observed no effect on Pma1 and Can1 sorting (Figure 6), further suggesting the *drs2*Δ missorting defect is not an indirect consequence of disrupting unrelated TGN trafficking pathways.

DISCUSSION

The experiments presented here show that PS flip by Drs2 at the yeast TGN regulates the lipid-based sorting of proteins into exocytic vesicles. Pma1 and Can1 populate nonoverlapping compartments of the plasma membrane, but partitioning into microdomains rich in ergosterol and sphingolipids is believed to concentrate both proteins into exocytic vesicles at the TGN (Klemm *et al.*, 2009; Surma *et al.*, 2012). Evidence of Drs2's involvement as a sorting factor in this pathway is that disrupting *DRS2* causes 25 and 40% of Pma1 and Can1 to missort to the vacuole (Figures 2, A and B, and 3, A and B), respectively. In addition, 20% of ergosterol appears to mislocalize to internal membranes in *drs2Δ* cells as assessed by filipin staining and DHE fluorescence (Figure 4, A–D). These defects are specific to loss of PS flip because Drs2-[QQ → GA], which loses the ability to flip PS without altering the ability to flip PE (Baldridge and Graham, 2013), causes mislocalization of Pma1-GFP, Can1-GFP, and ergosterol to the same extent as *drs2Δ*. In contrast, Dnf1-N550S, which gains the ability to flip PS without altering transport of its normal substrates, fully restores efficient sorting of Pma1-GFP, Can1-GFP, and ergosterol localization to the plasma membrane in *drs2Δ* cells. However, Pma1-RFP and Can1-GFP that arrive at the plasma membrane of *drs2Δ* cells segregate normally into distinct membrane compartments, despite aberrantly exposing PS in the outer (extracellular) leaflet (Figure 1; Chen *et al.*, 2006). Thus, lateral compartmentalization of the plasma membrane does not depend on PS transverse asymmetry.

Consistent with plasma membrane compartmentalization being unperturbed, the mislocalization of Pma1-GFP and Can1-GFP in

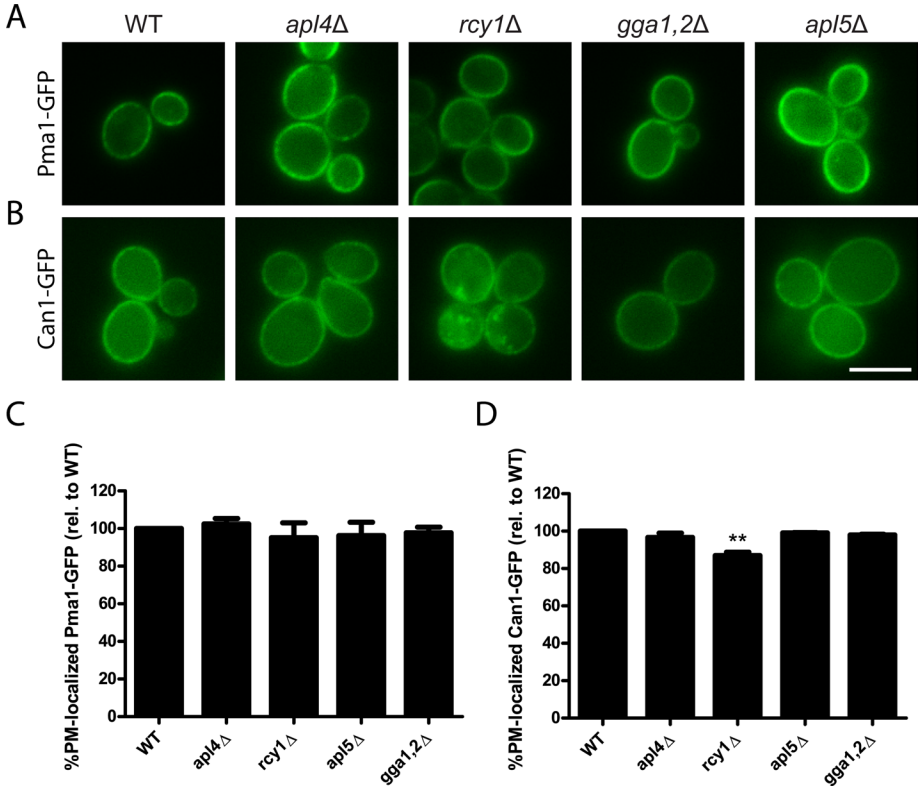

FIGURE 6: Missorting of Pma1 and Can1 is not due to disrupting other TGN-associated trafficking pathways. Cells expressing (A) Pma1-GFP or (B) Can1-GFP were grown to mid log phase at 30°C and imaged. Percentage of PM-localized (C) Pma1-GFP and (D) Can1-GFP were calculated by dividing plasma membrane fluorescence by total fluorescence with WT set to 100%. Values represent mean ± SEM ($n = 2$, total of 100 cells, one-way ANOVA, $^{**}p < 0.01$). Scale bar, 5 μm.

drs2Δ cells is due to a defect in sorting at the TGN rather than an increased rate of endocytosis. Blocking endocytosis had no effect on Pma1-GFP and Can1-GFP delivery to the vacuole (Figure 5), which would be expected if *drs2Δ* destabilized the residence of these proteins within separate plasma membrane compartments. Missorting of Pma1-GFP and Can1-GFP is also independent of known *drs2*Δ defects in bidirectional trafficking between the TGN and early endosomes (AP-1/clathrin and Rcy1 recycling pathways; Furuta *et al.*, 2007; Liu *et al.*, 2008), as disrupting these pathways had little to no effect on Pma1 and Can1 localization (Figure 6). We also observed no effect when we disrupted other TGN-associated trafficking pathways mediated by GGA and AP-3. These findings suggest that the Pma1-GFP and Can1-GFP missorting defects are not an indirect consequence of disrupting other coat-dependent TGN trafficking pathways but instead are a specific consequence of perturbing PS flip.

It is possible that failure to remove PS from the lumenal leaflet of the *drs2Δ* TGN disrupts the lipid-based segregation of plasma membrane proteins into regions of the membrane that are released from the TGN to become exocytic vesicles. This explanation is unlikely because *cho1Δ* cells, which lack PS, have the same degree of Can1-GFP and Pma1-GFP missorting as observed in *drs2* mutants (Figures 2, A and B, and 3, A and B). Moreover, deletion of *CHO1* was been shown to exacerbate, rather than suppress, *drs2* phenotypes (Natarajan *et al.*, 2004). These results suggest a positive role for PS in the formation of microdomains in the TGN rather than a poisoning of microdomain organization in the lumenal leaflet when PS is present in the flippase mutant. Whereas *cho1Δ* displayed substantial variability in ergosterol subcellular localization (Figure 4), these cells were uniformly defective in sorting Pma1 and Can1 (Figures 2, A and B, and 3, A and B). This observation again implies a positive role for PS in exocytic protein sorting that may be independent of sterol homeostasis. Therefore we suggest that it is either the physical displacement of PS across the TGN membrane or its appearance in the cytosolic leaflet that is crucial for concentrating Pma1 and Can1 into exocytic vesicles.

Translocation of PS across the TGN bilayer should have a number of effects on the biophysical properties of the membrane. The unidirectional movement of PS reduces the surface area of the inner (lumenal) leaflet while simultaneously expanding the outer (cytosolic) leaflet. This imbalance places stress on the membrane that can be relieved by membrane bending and budding of small-diameter vesicles (Sheetz and Singer, 1974; Graham, 2004). In addition, the PS head group carries a negative charge and also has an intrinsic positive curvature due to its conical shape that should accentuate membrane bending toward the cytosol (Fuller *et al.*, 2003). Consistent with this prediction, localization of a biosensor for membrane curvature and charge (+ALPS-GFP) to TGN and early endosomal membranes requires PS flip by Drs2 (Xu *et al.*, 2013). The induction of curvature by PS flip may be sufficient to facilitate sorting of lipids or proteins into subdomains of the TGN that give rise to exocytic vesicles (Roux *et al.*, 2005; Sorre *et al.*, 2009; Ryu *et al.*, 2014).

Another potential effect of unidirectional PS flip is that overcrowding the cytosolic leaflet could provide a driving force to push lipids that can spontaneously flip-flop, such as ergosterol, to the lumenal leaflet. Freeze-fracture electron microscopy studies of filipin-stained mammalian cells indicate that cholesterol moves in bulk across the bilayer to the lumenal leaflet during secretory granule formation (Orci *et al.*, 1980, 1981a,b). This movement of cholesterol may coincide with the bulk movement of PS from the lumenal to cytosolic leaflet at the TGN (Fairn *et al.*, 2011). In yeast, this interleaflet exchange of PS for ergosterol may sufficiently concentrate ergosterol and sphingolipid in the lumenal leaflet to induce domain formation and partitioning of plasma membrane proteins into these domains. Once nucleated from the lumenal leaflet, the preference of the Pma1 and Can1 membrane domains for ergosterol and saturated phospholipid may propagate the microdomain organization to the cytosolic leaflet. Exocytic vesicles in budding yeast are significantly enriched for ergosterol relative to the TGN membrane from which they were formed (Zinser *et al.*, 1991, 1993; Klemm *et al.*, 2009). The source of this additional ergosterol may be the OSBP homologue Kes1, which is capable of loading the TGN membrane (or newly budded vesicle) with ergosterol in exchange for PI4P (Mesmin *et al.*, 2013; von Filseck *et al.*, 2015).

Based on the present study, Drs2 and Kes1 are required for efficient sorting of Pma1 and Can1 to the plasma membrane. In the absence of PS flip or Kes1 activity, the TGN still buds exocytic

vesicles that are delivered normally to the plasma membrane; however, Pma1 and Can1 are not efficiently concentrated into these exocytic vesicles and likely spill into vesicles targeted to the endosomal system. Genetically, *DRS2* and *KES1* appear to antagonize each other's activity (Muthusamy *et al.*, 2009). Single mutants carrying *drs2Δ* or *kes1Δ* mutations display the same defect in Pma1 and Can1 localization, but the *drs2Δ kes1Δ* double mutant is indistinguishable from WT cells. This observation may seem to diminish the significance of flippases and OSBP homologues in this pathway, as they are dispensable; however, Drs2 and Kes1 are both members of large protein families with some degree of functional redundancy (seven OSBP homologues and five flippases are expressed in budding yeast). For instance, *kes1Δ* will suppress *drs2Δ* phenotypes, but it does not suppress the lethality caused by deletion of *DRS2* and the *DNF* genes (*drs2Δdnf1,2,3Δ*; Muthusamy *et al.*, 2009).

Our data suggest that it is critical to balance the activity of Drs2 and Kes1 during TGN membrane remodeling events to ensure correct sorting of proteins and lipids. Biochemical experiments support this idea: Drs2 PS flippase activity is twofold higher in Golgi membranes purified from *kes1Δ* cells relative to WT cells (Muthusamy *et al.*, 2009). Addition of recombinant Kes1 to *kes1Δ* Golgi membranes inhibited Drs2 to WT levels with $IC_{50} \approx 100$ fM (Muthusamy *et al.*, 2009). Inhibition was likely caused by the ability of Kes1 to extract PI4P from the TGN, which is a stimulator of Drs2 activity (Natarajan *et al.*, 2009; Zhou *et al.*, 2013). Conversely, high concentrations of PS inhibit the ability of Kes1 to exchange sterol for PI4P in transfer assays with liposomes, potentially by trapping Kes1 on the membrane and causing a futile cycle of exchange with the same membrane (Saint-Jean *et al.*, 2011). Thus Drs2-catalyzed PS translocation at the TGN may attenuate Kes1's ability to load ergosterol into the TGN. Therefore we suggest that Kes1 overloads the TGN with ergosterol in situations when Drs2 is absent, when Drs2 cannot recognize PS (Drs2-[QQ → GA]), or when Drs2 cannot flip PS because PS is absent (*cho1Δ* cells). The similar phenotypes of *kes1Δ* and *drs2Δ* single mutants imply that overloading or underloading the TGN with ergosterol disrupts the balance required for concentrating Pma1 and Can1 into microdomains for their selective incorporation into exocytic vesicles.

MATERIALS AND METHODS

Media, strains, and plasmids

Yeast strains were grown in synthetic minimal medium (SD) containing required nutrients and 2% glucose. For experiments involving *cho1*Δ, the SD medium was supplemented with 1 mM choline (Sigma-Aldrich, St. Louis, MO). All yeast transformations were performed by the lithium acetate method (Gietz and Schiestl, 2007). PCR-based genomic integration of fluorescent tags was carried out according to the method described by Janke *et al.* (2004). The strains and plasmids used in this study are listed in Supplemental Tables S1 and S2, respectively.

Western blot

Samples were prepared using a protocol modified from Chang and Slayman (1991). Cell pellets were resuspended in lysis buffer (10 mM Tris, pH 7.4, 0.3 M sorbitol, 0.1 M NaCl, and 5 mM $MgCl_2$) containing 1 mM phenylmethylsulfonyl fluoride and 1× protease inhibitor cocktail (ThermoFisher Scientific, San Jose, CA). The cells were then lysed by vortexing for 6 min with 1-min pulses at 4°C. The beads were allowed to settle without centrifugation for 10 min at 4°C before removing the lysate supernatant. The lysates were then added 1:1 to Laemmli buffer and incubated at 37°C for 5 min. The samples were then subjected to SDS–PAGE and transferred to a polyvinylidene fluoride membrane. For the anti-GFP Western blot, an IR800CW secondary antibody was used, and the bands were imaged and quantified using an Odyssey CLx infrared imager and its software (LI-COR Biosciences, Lincoln, NE).

Vacuolar labeling with FM4-64

To confirm vacuolar localization of GFP-tagged Pma1 and Can1, mid log-phase (OD_{600} = 0.5–0.8) cells were labeled with the lipophilic dye FM4-64 (Life Technologies, Grand Island, NY) as described previously (Babu *et al.*, 2012). Cells were labeled with 32 μM FM4-64 for 20 min in the dark at 30°C. The cells were then washed with 1× phosphate-buffered saline (PBS) and resuspended in SD medium for 30 min at 30°C. The cells were washed twice in 1× PBS before imaging.

Filipin staining

To examine the distribution of ergosterol, cells were stained with filipin (Sigma-Aldrich) using a protocol similar to the one described by Beh and Rine (2004). A 5-ml amount of mid log-phase (OD_{600} = 0.5–0.8) cells grown in SD medium was fixed with 4% formaldehyde for 10 min at 30°C with shaking. The cells were then harvested and washed twice with 10 ml of sterile water. The cells were resuspended in 1 ml of sterile water, 0.2 ml of which was mixed with 3 μl of freshly prepared, ice-cold 5 mg/ml filipin in ethanol. The cells were then incubated with filipin for 15 min at 30°C in the dark before harvesting the cells and imaging.

Dehydroergosterol uptake assay

DHE (Sigma-Aldrich), a naturally occurring fluorescent sterol (McIntosh *et al.*, 2008), was used to visualize the distribution of ergosterol in living cells. Yeast strains were incubated with DHE under hypoxic conditions to allow for sterol uptake and imaged as described previously (Georgiev *et al.*, 2011; Gatta *et al.*, 2015). Briefly, yeast strains were inoculated from an overnight saturated liquid culture to $OD_{600} \approx 0.005$ in 10 ml of synthetic medium supplemented with 20 μg/ml DHE, 0.5% ethanol, and 0.5% Tween-80. The cultures, together with BD GasPak EZ Anaerobe carbon sachets (BD Diagnostics, Franklin Lakes, NJ), were placed inside an anaerobe incubation chamber, and the chamber was then sealed and incubated at 30°C for 36 h. The sachets reduce oxygen levels to 0.7% (vol/vol), yielding hypoxic conditions. At the end of the hypoxic incubation, the chamber was opened, and cells were energy poisoned with ice-cold NaN_3/NaF (10 mM/10 mM) before imaging.

Sucrose gradient fractionation

Cell homogenates were analyzed by sucrose gradient fractionation as previously described (Georgiev *et al.*, 2011; Gatta *et al.*, 2015). Seven fractions were collected from the top of the gradient, and each fraction was immunoblotted against Dpm1 (ER marker) and Pma1 (plasma membrane marker) to verify that the fractionation was successful.

Actin depolymerization

Lat A (Cayman Chemical, Ann Arbor, MI) was used to block endocytosis through inhibition of actin polymerization. Mid log-phase (OD_{600} = 0.5–0.8) cells were harvested, resuspended in SD medium containing 10 μM Lat A, and incubated for 3 h at 30°C as described previously (Huang and Chang, 2011). Control cells were treated with an equal volume of ethanol.

Induction of Can1 endocytosis with arginine

Can1 endocytosis was triggered by the addition of arginine as described by Brach *et al*. (2011). Cells were grown to OD = 0.4, harvested, and resuspended in SD medium supplemented with 5 mM arginine. Cells were incubated for 3 h at 30°C before imaging.

Fluorescence microscopy

Images of Pma1-RFP and Can1-GFP distribution at the plasma membrane were taken with a DeltaVision Elite Imaging system (Applied Precision, Issaquah, WA). A *Z*-stack was acquired with 200-nm intervals, and the images were deconvolved in SoftWoRx (Applied Precision, Issaquah, WA). Images of DHE were taken with an inverted microscope (Leica, Deerfield, IL) equipped with a cooled charge-coupled device camera (Princeton Instruments, Trenton, NJ) and MetaMorph software (Universal Imaging, West Chester, PA). To visualize DHE, a specially designed filter cube (Chroma Technology, Brattleboro, VT) was used with a 355-nm (20-nm bandpass) excitation filter, a 365-nm long-pass dichromatic filter, and a 405-nm (40-nm bandpass) emission filter. All other images were taken with an Axioplan microscope (Carl Zeiss, Thornwood, NY) equipped with a Zyla sCMOS 5.5-megapixel camera (Andor, Belfast, United Kingdom) and micromanager software (University of California, San Francisco, San Francisco, CA). Filipin was imaged using a 4′,6-diamidino-2-phenylindole filter set; GFP-tagged proteins were imaged using a GFP filter set; RFP-tagged proteins and FM4-64 were imaged using an RFP filter set. Images were merged and pseudocolored in ImageJ (National Institutes of Health, Bethesda, MD).

Data analysis

The percentage of filipin/Pma1/Can1/Snc1 localized to the plasma membrane (%PM-localized) was calculated by first outlining the outside of each cell using the freehand selection tool in ImageJ and measuring the total fluorescence of the cell ($Fluor_{Total}$). Next the area just within the plasma membrane was outlined using the freehand selection tool to give the total internal fluorescence excluding the plasma membrane ($Fluor_{int}$). Next the internal fluorescence was subtracted from the total to determine the fluorescence at the plasma membrane ($Fluor_{Total} - Fluor_{int} = Fluor_{PM}$). Finally, the fluorescence at the plasma membrane was divided by the total fluorescence of the cell to give %PM-localized fluorescence ($Fluor_{PM}/Fluor_{Total}$ = %PM-localized). All quantification was performed using raw images. To determine the degree of colocalization between Pma1-RFP and Can1-GFP at the plasma membrane, individual cells taken from one slice of a deconvolved Z-stack were outlined using the freehand selection tool in ImageJ and copied into new images to produce two images, one in the GFP channel and one in the RFP channel. The ImageJ plug-in Colocalization Finder (rsb.info.nih.gov/ij/plugins/colocalization-finder.html) was then used to calculate Pearson's coefficient for each cell.

ACKNOWLEDGMENTS

We thank Jason MacGurn, Scott Emr, Christopher Burd, and Roland Wedlich-Söldner for generously gifting us plasmids used in this study. We thank Fred Maxfield for the use of a fluorescence microscope to visualize DHE. We also thank Barbara O'Brien of the Vanderbilt University Medical Center Editors' Club for assistance with editing. Support for this project in the Menon lab was provided by the Qatar National Research Fund (NPRP 7-082-1-014). Research in the Graham lab is supported by a grant from the National Institutes of Health (1R01GM107978).

REFERENCES

Alfaro G, Johansen J, Dighe SA, Duamel G, Kozminski KG, Beh CT (2011). The sterol-binding protein Kes1/Osh4p is a regulator of polarized exocytosis. Traffic 12, 1521–1536.

Atkinson KD, Jensen B, Kolat AI, Storm EM, Henry SA, Fogel S (1980). Yeast mutants auxotrophic for choline or ethanolamine. J Bacteriol 141, 558–564.

Babu M, Vlasblom J, Pu S, Guo X, Graham C, Bean BDM, Burston HE, Vizeacoumar FJ, Snider J, Phanse S, *et al*. (2012). Interaction landscape of membrane-protein complexes in Saccharomyces cerevisiae. Nature 489, 585–589.

Bagnat M, Chang A, Simons K (2001). Plasma membrane proton ATPase Pma1p requires raft association for surface delivery in yeast. Mol Biol Cell 12, 4129–4138.

Bagnat M, Keränen S, Shevchenko A, Shevchenko A, Simons K (2000). Lipid rafts function in biosynthetic delivery of proteins to the cell surface in yeast. Proc Natl Acad Sci USA 97, 3254–3259.

Baldridge RD, Graham TR (2012). Identification of residues defining phospholipid flippase substrate specificity of type IV P-type ATPases. Proc Natl Acad Sci USA 109, E290–E298.

Baldridge RD, Graham TR (2013). Two-gate mechanism for phospholipid selection and transport by type IV P-type ATPases. Proc Natl Acad Sci USA 110, E358–E367.

Baldridge RD, Xu P, Graham TR (2013). Type IV P-type ATPases distinguish mono- versus diacyl phosphatidylserine using a cytofacial exit gate in the membrane domain. J Biol Chem 288, 19516–19527.

Beh CT, Rine J (2004). A role for yeast oxysterol-binding protein homologs in endocytosis and in the maintenance of intracellular sterol-lipid distribution. J Cell Sci 117, 2983–2996.

Brach T, Specht T, Kaksonen M (2011). Reassessment of the role of plasma membrane domains in the regulation of vesicular traffic in yeast. J Cell Sci 124, 328–337.

Chang A, Fink GR (1995). Targeting of the yeast plasma membrane [H+] ATPase: a novel gene AST1 prevents mislocalization of mutant ATPase to the vacuole. J Cell Biol 128, 39–49.

Chang A, Slayman CW (1991). Maturation of the yeast plasma membrane [H+]ATPase involves phosphorylation during intracellular transport. J Cell Biol 115, 289–295.

Chen C-Y, Ingram MF, Rosal PH, Graham TR (1999). Role for Drs2p, a P-type ATPase and potential aminophospholipid translocase, in yeast late Golgi function. J Cell Biol 147, 1223–1236.

Chen S, Wang J, Muthusamy B-P, Liu K, Zare S, Andersen RJ, Graham TR (2006). Roles for the Drs2p–Cdc50p complex in protein transport and phosphatidylserine asymmetry of the yeast plasma membrane. Traffic 7, 1503–1517.

Drabikowski W, Łagwińska E, Sarzała MG (1973). Filipin as a fluorescent probe for the location of cholesterol in the membranes of fragmented sarcoplasmic reticulum. Biochim Biophys Acta 291, 61–70.

Fairn GD, Schieber NL, Ariotti N, Murphy S, Kuerschner L, Webb RI, Grinstein S, Parton RG (2011). High-resolution mapping reveals topologically distinct cellular pools of phosphatidylserine. J Cell Biol 194, 257–275.

Fang M, Kearns BG, Gedvilaite A, Kagiwada S, Kearns M, Fung MK, Bankaitis VA (1996). Kes1p shares homology with human oxysterol binding protein and participates in a novel regulatory pathway for yeast Golgi-derived transport vesicle biogenesis. EMBO J 15, 6447–6459.

Fei W, Alfaro G, Muthusamy B-P, Klaassen Z, Graham TR, Yang H, Beh CT (2008). Genome-wide analysis of sterol-lipid storage and trafficking in Saccharomyces cerevisiae. Eukaryot Cell 7, 401–414.

Fuller N, Benatti CR, Rand RP (2003). Curvature and bending constants for phosphatidylserine-containing membranes. Biophys J 85, 1667–1674.

Furuta N, Fujimura-Kamada K, Saito K, Yamamoto T, Tanaka K (2007). Endocytic recycling in yeast is regulated by putative phospholipid translocases and the Ypt31p/32p–Rcy1p pathway. Mol Biol Cell 18, 295–312.

Gaigg B, Toulmay A, Schneiter R (2006). Very long-chain fatty acid-containing lipids rather than sphingolipids per se are required for raft association and stable surface transport of newly synthesized plasma membrane ATPase in yeast. J Biol Chem 281, 34135–34145.

Galan J-M, Wiederkehr A, Seol JH, Haguenauer-Tsapis R, Deshaies RJ, Riezman H, Peter M (2001). Skp1p and the F-Box protein Rcy1p form a non-SCF complex involved in recycling of the SNARE Snc1p in yeast. Mol Cell Biol 21, 3105–3117.

Gall WE, Geething NC, Hua Z, Ingram MF, Liu K, Chen SI, Graham TR (2002). Drs2p-dependent formation of exocytic clathrin-coated vesicles in vivo. Curr Biol 12, 1623–1627.

Gatta AT, Wong LH, Sere YY, Calderón-Noreña DM, Cockcroft S, Menon AK, Levine TP (2015). A new family of StART domain proteins at membrane contact sites has a role in ER-PM sterol transport. Elife 4, eLife.07253.
Georgiev AG, Sullivan DP, Kersting MC, Dittman JS, Beh CT, Menon AK (2011). Osh proteins regulate membrane sterol organization but are not required for sterol movement between the ER and PM. Traffic 12, 1341–1355.
Gietz RD, Schiestl RH (2007). High-efficiency yeast transformation using the LiAc/SS carrier DNA/PEG method. Nat Protoc 2, 31–34.
Graham TR (2004). Flippases and vesicle-mediated protein transport. Trends Cell Biol 14, 670–677.
Graham TR, Burd CG (2011). Coordination of Golgi functions by phosphatidylinositol 4-kinases. Trends Cell Biol 21, 113–121.
Grossmann G, Opekarova M, Malinsky J, Weig-Meckl I, Tanner W (2007). Membrane potential governs lateral segregation of plasma membrane proteins and lipids in yeast. EMBO J 26, 1–8.
Grossmann G, Opekarova M, Novakova L, Stolz J, Tanner W (2006). Lipid raft-based membrane compartmentation of a plant transport protein expressed in Saccharomyces cerevisiae. Eukaryot Cell 5, 945–953.
Gu F, Crump CM, Thomas G (2001). Trans-Golgi network sorting. Cell Mol Life Sci 58, 1067–1084.
Hankins HM, Baldridge RD, Xu P, Graham TR (2015). Role of flippases, scramblases and transfer proteins in phosphatidylserine subcellular distribution. Traffic 16, 35–47.
Hua Z, Fatheddin P, Graham TR (2002). An essential subfamily of Drs2p-related P-type ATPases is required for protein trafficking between Golgi complex and endosomal/vacuolar system. Mol Biol Cell 13, 3162–3177.
Huang C, Chang A (2011). pH-dependent cargo sorting from the Golgi. J Biol Chem 286, 10058–10065.
Ikonen E, Simons K (1998). Protein and lipid sorting from the trans-Golgi network to the plasma membrane in polarized cells. Semin Cell Dev Biol 9, 503–509.
Im YJ, Raychaudhuri S, Prinz WA, Hurley JH (2005). Structural mechanism for sterol sensing and transport by OSBP-related proteins. Nature 437, 154–158.
Janke C, Magiera MM, Rathfelder N, Taxis C, Reber S, Maekawa H, Moreno-Borchart A, Doenges G, Schwob E, Schiebel E, *et al*. (2004). A versatile toolbox for PCR-based tagging of yeast genes: new fluorescent proteins, more markers and promoter substitution cassettes. Yeast 21, 947–962.
Jiang B, Brown JL, Sheraton J, Fortin N, Bussey H (1994). A new family of yeast genes implicated in ergosterol synthesis is related to the human oxysterol binding protein. Yeast 10, 341–353.
Kato U, Emoto K, Fredriksson C, Nakamura H, Ohta A, Kobayashi T, Murakami-Murofushi K, Kobayashi T, Umeda M (2002). A novel membrane protein, Ros3p, is required for phospholipid translocation across the plasma membrane in Saccharomyces cerevisiae. J Biol Chem 277, 37855–37862.
Kelley MJ, Bailis AM, Henry SA, Carman GM (1988). Regulation of phospholipid biosynthesis in Saccharomyces cerevisiae by inositol. Inositol is an inhibitor of phosphatidylserine synthase activity. J Biol Chem 263, 18078–18085.
Klemm RW, Ejsing CS, Surma MA, Kaiser H-J, Gerl MJ, Sampaio JL, Robillard Q de, Ferguson C, Proszynski TJ, Shevchenko A, *et al*. (2009). Segregation of sphingolipids and sterols during formation of secretory vesicles at the trans-Golgi network. J Cell Biol 185, 601–612.
Lewis MJ, Nichols BJ, Prescianotto-Baschong C, Riezman H, Pelham HR B (2000). Specific retrieval of the exocytic SNARE Snc1p from early yeast endosomes. Mol Biol Cell 11, 23–38.
Li X, Rivas MP, Fang M, Marchena J, Mehrotra B, Chaudhary A, Feng L, Prestwich GD, Bankaitis VA (2002). Analysis of oxysterol binding protein homologue Kes1p function in regulation of Sec14p-dependent protein transport from the yeast Golgi complex. J Cell Biol 157, 63–78.
Liu K, Surendhran K, Nothwehr SF, Graham TR (2008). P4-ATPase requirement for AP-1/clathrin function in protein transport from the trans-Golgi network and early endosomes. Mol Biol Cell 19, 3526–3535.
Luo W, Chang A (2000). An endosome-to-plasma membrane pathway involved in trafficking of a mutant plasma membrane ATPase in yeast. Mol Biol Cell 11, 579–592.
Malínská K, Malínský J, Opekarová M, Tanner W (2003). Visualization of protein compartmentation within the plasma membrane of living yeast cells. Mol Biol Cell 14, 4427–4436.
Malinska K, Malinsky J, Opekarova M, Tanner W (2004). Distribution of Can1p into stable domains reflects lateral protein segregation within the plasma membrane of living S. cerevisiae cells. J Cell Sci 117, 6031–6041.
Maxfield FR, Wüstner D (2012). Analysis of cholesterol trafficking with fluorescent probes. Methods Cell Biol 108, 367–393.
McIntosh AL, Atshaves BP, Huang H, Gallegos AM, Kier AB, Schroeder F (2008). Fluorescence techniques using dehydroergosterol to study cholesterol trafficking. Lipids 43, 1185–1208.
Mesmin B, Bigay J, Moser von Filseck J, Lacas-Gervais S, Drin G, Antonny B (2013). A four-step cycle driven by PI(4)P hydrolysis directs sterol/PI(4)P exchange by the ER-Golgi tether OSBP. Cell 155, 830–843.
Moser von Filseck J, Vanni S, Mesmin B, Antonny B, Drin G (2015). A phosphatidylinositol-4-phosphate powered exchange mechanism to create a lipid gradient between membranes. Nat Commun 6, 6671.
Muthusamy B-P, Raychaudhuri S, Natarajan P, Abe F, Liu K, Prinz WA, Graham TR (2009). Control of protein and sterol trafficking by antagonistic activities of a type IV P-type ATPase and oxysterol binding protein homologue. Mol Biol Cell 20, 2920–2931.
Natarajan P, Liu K, Patil DV, Sciorra VA, Jackson CL, Graham TR (2009). Regulation of a Golgi flippase by phosphoinositides and an ArfGEF. Nat Cell Biol 11, 1421–1426.
Natarajan P, Wang J, Hua Z, Graham TR (2004). Drs2p-coupled aminophospholipid translocase activity in yeast Golgi membranes and relationship to in vivo function. Proc Natl Acad Sci USA 101, 10614–10619.
Norman AW, Demel RA, Kruyff B de, Deenen LLM van (1972). Studies on the biological properties of polyene antibiotics. Evidence for the direct interaction of filipin with cholesterol. J Biol Chem 247, 1918–1929.
Odorizzi G, Babst M, Emr SD (1998). Fab1p PtdIns(3)P 5-kinase function essential for protein sorting in the multivesicular body. Cell 95, 847–858.
Opekarová M, Malínská K, Nováková L, Tanner W (2005). Differential effect of phosphatidylethanolamine depletion on raft proteins: further evidence for diversity of rafts in Saccharomyces cerevisiae. Biochim Biophys Acta 1711, 87–95.
Orci L, Amherdt M, Montesano R, Vassalli P, Perrelet A (1981a). Topology of morphologically detectable protein and cholesterol in membranes of polypeptide-secreting cells. Philos Trans R Soc Lond B Biol Sci 296, 47–54.
Orci L, Miller RG, Montesano R, Perrelet A, Amherdt M, Vassalli P (1980). Opposite polarity of filipin-induced deformations in the membrane of condensing vacuoles and zymogen granules. Science 210, 1019–1021.
Orci L, Montesano R, Meda P, Malaisse-Lagae F, Brown D, Perrelet A, Vassalli P (1981b). Heterogeneous distribution of filipin–cholesterol complexes across the cisternae of the Golgi apparatus. Proc Natl Acad Sci USA 78, 293–297.
Papanikou E, Glick BS (2014). Golgi compartmentation and identity. Curr Opin Cell Biol 29, 74–81.
Pomorski T, Lombardi R, Riezman H, Devaux PF, van Meer G, Holthuis JC (2003). Drs2p-related P-type ATPases Dnf1p and Dnf2p are required for phospholipid translocation across the yeast plasma membrane and serve a role in endocytosis. Mol Biol Cell 14, 1240–1254.
Prosser DC, Whitworth K, Wendland B (2010). Quantitative analysis of endocytosis with cytoplasmic pHluorin chimeras. Traffic 11, 1141–1150.
Proszynski TJ, Klemm RW, Gravert M, Hsu PP, Gloor Y, Wagner J, Kozak K, Grabner H, Walzer K, Bagnat M, *et al*. (2005). A genome-wide visual screen reveals a role for sphingolipids and ergosterol in cell surface delivery in yeast. Proc Natl Acad Sci USA 102, 17981–17986.
Riekhof WR, Wu J, Gijón MA, Zarini S, Murphy RC, Voelker DR (2007). Lysophosphatidylcholine metabolism in Saccharomyces cerevisiae. The role of P-type ATPases in transport and a broad specificity acyltransferase in acylation. J Biol Chem 282, 36853–36861.
Robinson MS (2004). Adaptable adaptors for coated vesicles. Trends Cell Biol 14, 167–174.
Roux A, Cuvelier D, Nassoy P, Prost J, Bassereau P, Goud B (2005). Role of curvature and phase transition in lipid sorting and fission of membrane tubules. EMBO J 24, 1537–1545.
Ryu Y-S, Lee I-H, Suh J-H, Park SC, Oh S, Jordan LR, Wittenberg NJ, Oh S-H, Jeon NL, Lee B, *et al*. (2014). Reconstituting ring-rafts in bud-mimicking topography of model membranes. Nat Commun 5, 4507.

Saint-Jean M de, Delfosse V, Douguet D, Chicanne G, Payrastre B, Bourguet W, Antonny B, Drin G (2011). Osh4p exchanges sterols for phosphatidylinositol 4-phosphate between lipid bilayers. J Cell Biol 195, 965–978.
Saito K, Fujimura-Kamada K, Furuta N, Kato U, Umeda M, Tanaka K (2004). Cdc50p, a protein required for polarized growth, associates with the Drs2p P-Type ATPase implicated in phospholipid translocation in Saccharomyces cerevisiae. Mol Biol Cell 15, 3418–3432.
Sheetz MP, Singer SJ (1974). Biological membranes as bilayer couples. A molecular mechanism of drug-erythrocyte interactions. Proc Natl Acad Sci USA 71, 4457–4461.
Simons K, Ikonen E (1997). Functional rafts in cell membranes. Nature 387, 569–572.
Simons K, van Meer G (1988). Lipid sorting in epithelial cells. Biochemistry 27, 6197–6202.
Sorre B, Callan-Jones A, Manneville J-B, Nassoy P, Joanny J-F, Prost J, Goud B, Bassereau P (2009). Curvature-driven lipid sorting needs proximity to a demixing point and is aided by proteins. Proc Natl Acad Sci USA 106, 5622–5626.
Spira F, Mueller NS, Beck G, von Olshausen P, Beig J, Wedlich-Söldner R (2012). Patchwork organization of the yeast plasma membrane into numerous coexisting domains. Nat Cell Biol 14, 640–648.
Surma MA, Klose C, Simons K (2012). Lipid-dependent protein sorting at the trans-Golgi network. Biochim Biophys Acta 1821, 1059–1067.
Takahashi Y, Fujimura-Kamada K, Kondo S, Tanaka K (2011). Isolation and characterization of novel mutations in CDC50, the noncatalytic subunit of the Drs2p phospholipid flippase. J Biochem 149, 423–432.
Umebayashi K, Nakano A (2003). Ergosterol is required for targeting of tryptophan permease to the yeast plasma membrane. J Cell Biol 161, 1117–1131.
Xu P, Baldridge RD, Chi RJ, Burd CG, Graham TR (2013). Phosphatidylserine flipping enhances membrane curvature and negative charge required for vesicular transport. J Cell Biol 202, 875–886.
Zhou X, Sebastian TT, Graham TR (2013). Auto-inhibition of Drs2p, a yeast phospholipid flippase, by its carboxyl-terminal tail. J Biol Chem 288, 31807–31815.
Zinser E, Paltauf F, Daum G (1993). Sterol composition of yeast organelle membranes and subcellular distribution of enzymes involved in sterol metabolism. J Bacteriol 175, 2853–2858.
Zinser E, Sperka-Gottlieb CD, Fasch EV, Kohlwein SD, Paltauf F, Daum G (1991). Phospholipid synthesis and lipid composition of subcellular membranes in the unicellular eukaryote Saccharomyces cerevisiae. J Bacteriol 173, 2026–2034.
Ziółkowska NE, Christiano R, Walther TC (2012). Organized living: formation mechanisms and functions of plasma membrane domains in yeast. Trends Cell Biol 22, 151–158.